

Heterogeneous and Homogeneous Reactions of Pyrolysis Vapors from Pine Wood

Elly Hoekstra, Roel J. M. Westerhof, Wim Brilman, Wim P.M. Van Swaaij, Sascha R. A. Kersten, and Kees J. A. Hogendoorn

University of Twente, Faculty of Science and Technology, P.O. Box 217, 7500 AE Enschede, The Netherlands

Michael Windt

vTI-Institute of Wood Technology and Wood Biology, Leuschnerstr. 91, 21031 Hamburg, Germany

DOI 10.1002/aic.12799

Published online November 30, 2011 in Wiley Online Library (wileyonlinelibrary.com).

To maximize oil yields in the fast pyrolysis of biomass it is generally accepted that vapors need to be rapidly quenched. The influence of the heterogeneous and homogeneous vapor-phase reactions on yields and oil composition were studied using a fluidized-bed reactor. Even high concentrations of mineral low char (till 55 vol %) appeared not to be catalytically active. However, the presence of minerals, either in biomass or added, does influence the yields, especially by the occurrence of vapor-phase charring/polymerization reactions. Contradictory, in the absence of minerals, homogeneous vapor-phase cracking reactions were dominant over polymerization/charring reactions (400–550°C, 1–15 s). With increasing vapor residence time, the oil yield reached an asymptotic value, which decreased with temperature. At a vapor temperature of 400°C no decrease in oil yield was observed, but dedicated analysis showed that homogeneous vapor to vapor reactions had occurred. © 2011 American Institute of Chemical Engineers AIChE J, 58: 2830–2842, 2012

Keywords: fast pyrolysis, reaction mechanism, biomass, vapor phase, minerals

Introduction

Fast pyrolysis is the thermochemical decomposition of organic material (moisture content typically <10 wt %) at 400–600°C in the absence of oxygen.^{1–3} In this process, biomass is converted into char (typically 15–25 wt %), permanent gases (typically 10–20 wt %) and pyrolysis oil (typically 60–70 wt %).^{1–3} Besides direct use for combustion³ and flavor production⁴ pyrolysis oil is considered to be an intermediate to be used in subsequent processes.⁴ For example, pyrolysis oil could be (1) upgraded so the resulting oil can be core fined in a standard refinery unit to (blending compounds for) fuels,³ (2) gasified to syngas followed by Fischer Tropsch synthesis to fuels/waxes or methanol synthesis,^{2,4} and (3) used as source for the extraction of chemicals (glycoaldehyde, levoglucosan, phenolics).^{3,4} The potential of fast pyrolysis as biomass pretreatment step is directly related to the significantly higher density of the oil (~1,200 kg/m³) compared to the original biomass (~150 kg/m³) and the resulting transportations benefits.^{2,4}

Pyrolysis oil is a mixture of water and hundreds of (oxygenated) organic compounds.¹ Over the past 3 decades, extensive research on the development of fast pyrolysis processes has been carried out. In order to obtain high-oil yields it is generally accepted that (1) high-heating rates are required, (2) the pyrolysis reaction temperature needs to be

controlled around 500°C, and (3) pyrolysis vapors/aerosols need to be rapidly quenched (<2 s).^{1,5–7} In the last decade increased fundamental insight in pyrolysis has been obtained^{8–13} with also quite some experimentally observed exceptions to the aforementioned general design rules.^{10,11,13} For example, Scott et al.¹³ found no significant influence of the vapor residence time on oil yields at up to 10 s, and temperatures between 400 and 450°C. A critical assessment of the “design rules”, their theoretical background and experimental verification seems, therefore, appropriate.

Pyrolysis products are formed by decomposition reactions of the biomass matrix (cellulose, hemicellulose, and lignin) followed by reactions of produced gases, vapors, aerosols, liquids and solids. The vapors and aerosols form, after condensation, the liquid product called “pyrolysis oil” or “bio-oil”. In our experiments, it is not known what the nature of the oil is at the pyrolysis temperature, viz. vapors, aerosols or a combination of those. In the remainder of the text, both vapors and aerosols are denoted as vapors, but the reader should realize that “vapors” represent any combination of vapors and aerosols. Reactions of vapors are known to reduce the oil yield^{14–21} by both homogeneous and heterogeneous reaction pathways. However, there is only limited information on the effect of these reactions on the oil composition.^{15,21} Heterogeneous reactions can proceed when produced vapors leave the reacting biomass particle, vapors encounter other particles (char, ash, catalysts) or when vapors are in contact with the (hot) reactor material. The extent of vapor reactions is reported to depend, among others, on the temperature of the vapor phase, on the nature

Correspondence concerning this article should be addressed to R. J. M. Westerhof at R.J.M.Westerhof@utwente.nl.

Table 1. Biomass Properties

	Pine Wood	Pine Wood + KCl	Straw
ash [wt% _{dry}]	0.6	1.34	6.0
C [wt% _{dar}]	47.9	47.9	49.8
H [wt% _{dar}]	5.9	5.9	6.0
O [wt% _{dar}]	46.2	46.2	44.2
Water [wt%]	2–10	0.7	0.4
K [ppm _{dry}]	4.0E+02	6.5E+03	1.2E+04
Na [ppm _{dry}]	1.0E+02	1.0E+02	8.5E+1
Particle size [mm]	~ 1	~ 1	length < 5 mm

of the solid surfaces and the exposure time to high temperatures and/or surfaces,^{14–21} but possibly on the concentration of the vapors as well.^{15,22} Some researchers reported a significant influence of the presence of char on the extent of heterogeneous vapor-phase reactions,^{14,23} while others did not observe such an influence.¹⁰ The controversies in these results are probably related to (1) char composition, and (2) difficulties in separating the individual effects of biomass decomposition and homogeneous and heterogeneous vapor-phase reactions while interpreting the results.

The objective of this study is to obtain more unequivocal insight on the influence of (a) the vapor-phase residence time and temperature, and (b) char and minerals, on the oil yield and composition. In the last part of this article, the results are discussed in relation to kinetic model development and the engineering aspects of pyrolysis units.

Equipment and Procedure

Feedstock materials

The feedstock materials used and their properties are summarized in Table 1. Pine wood with a low-mineral content (Lignocel 9, purchased from Rettenmaier and Sohne GmbH, Germany) was used for the majority of the experiments. Some experiments were carried out with feedstocks high in mineral content. The presence of potassium is known to have a strong effect on the pyrolysis process.^{7,29,30} For this reason we have chosen to impregnate pine wood with KCl (Sigma, P9333, purity >99.0%) by mixing pine wood rigorously with a KCl solution and, subsequently, evaporating the water. Straw (purchased from DIVRO) was used as biomass which, by nature, has a high mineral and especially potassium content.

Pilot plant: analysis of in-bed char and minerals

A fluidized sand bed fast pyrolysis unit was used to study the effect of char and mineral holdup in the bed. The

reported char and mineral holdups (vol % and wt %) are expressed on total solid (char + sand + minerals) basis. The setup consisted of a continuous feeding system (0.5–0.9 kg/h), a fluidized-bed reactor (<200 d_{sand} <300 μm), three cyclones and a condensation train (spray column and intensive cooler) placed in series. The complete setup including a comprehensive validation is described in detail elsewhere.^{11,31} The standard deviations for the char, gas, oil and water yield were 1.0, 0.9, 1.3 and 1.0 wt %, respectively showing that the reproducibility of the experiments is good.³¹ Information about the operating conditions is listed in Tables 2 and 3. This setup will further be referred to as “pilot-plant”.

In the pilot plant it was possible to control the char and mineral holdup during the course of an experiment. A schematic overview of the reactor including the char/mineral holdup regulation system is shown in Figure 1. The fluidized-bed reactor ($D = 10$ cm, $H = 40$ cm) was equipped with an overflow to remove the sand/char/mixture mixture on top of the bed to keep the bed level constant ($V_{\text{reactor}} = 1.8$ L). Biomass and sand were fed by two separate feeding screws. Additives like minerals and char could be added to the sand flow. The amount of char and minerals inside the fluidized-bed reactor was controlled by adapting the sand/additives composition and feeding rate and by the biomass type and feeding rate. It was assumed that all solids in the fluidized bed were ideally mixed. For the “20 vol % char” experiment (estimated value, based on assumption ideal mixing), the char holdup inside the fluidized-bed reactor was experimentally determined after the experiment to validate the assumption. A value of 19 vol % was obtained which shows good agreement. Cold-flow experiments did show that it was possible to fluidize sand/char mixtures up to 63 vol % of char so no problems concerning the fluidization behavior/mixing were to be expected during our experiments (up to 55 vol % char).

Fluidized bed with tubular reactor placed in series (FB+T-Reactor): analysis of homogeneous vapor reactions

Setups used in Literature. In literature, a variety of setups is reported to have been used to study homogeneous pyrolysis vapor reactions. Although interesting results were obtained, many of the setups had some limitations making interpretation and extrapolation of results difficult. In several studies a batch type of pyrolysis reactor was coupled to a tubular reactor making continuous operation of the tubular reactor impossible.^{14,15,17,18,32,33} In literature the vapor residence times was varied either by changing the carrier

Table 2. Experimental Specification for Experiments in Pilot Plant ($T \sim 450$ – 490°C)

Name	Biomass*	Additives	Char Hold-Up [vol%]		K+ Na Hold-Up [wt%]**
			Pine	Straw	
20 vol% char	pine	none	20	0	0.005
55 vol% char	pine	none	55	0	0.021
KCl impregnated	KCl ^a , pine	none	50	0	0.176
straw	straw	none	0	35	0.167
Na/K additive 0.7 wt%	pine	Na ₂ CO ₃ ^b , K ₂ CO ₃ ^c	40	0	0.709
Na/K additive 0.1 wt%	pine	Na ₂ CO ₃ ^b , K ₂ CO ₃ ^c	31	0	0.110
straw char additive	pine	straw char	25	20	0.111

*Properties listed in Table 1, and

**mineral is minerals char plus minerals additives

^aSigma-Aldrich, P9333, purity > 99.0%,

^bSigma-Aldrich S7795, purity > 99.0%,

^cSigma-Aldrich 23653-412 K₂CO₃, purity = 99.0%

Table 3. Operating Conditions Pilot Plant and Lab-Scale Fluidized-Bed Reactor

	Properties	Pilot Plant	FB+T-reactor
General	Experimental Run Time [min]	90-120	60
Feeding	$\Phi_{m,sand}$ [kg/hr]	1.6-4.1	No sand fed to reactor
	$\Phi_{m,biomass}$ [kg/hr]	0.5-0.9	0.15
Fluidized bed reactor	$\Phi_{v,N_2} / \Phi_{m,biomass}$ [Nl/g]	~ 2.5	~ 4.5
	Char Hold-Up [vol%]	20-55 (\sim stationary)	0-25 (increasing)
	$T_{reactor}$ [$^{\circ}$ C]	400-530	500
	Φ_{vapors} [s]	1.6-1.9	~ 1.5
	$\Phi_{particles}$ [min]	20-40 min	No removal of particles
	U / U_{mf} [-]	4	3
Tubular reactor	Char separation	three cyclones in series	9 μ m and 5 μ m filters in series
	$T_{tube\ system}$ [$^{\circ}$ C]	no tubular reactor incorporated	400, 500, 550
	$T_{tube\ system}$ [s]		1.1-15.3
	Vapors + gases [vol%]		~ 9
	Re [-]		~ 275 -385
	Pe [-]		~ 20 -260
Condensation System	$T_{first\ condensor}$ [$^{\circ}$ C]	20 (spray column)	< 24 (ESP)
	$T_{second\ condensor}$ [$^{\circ}$ C]	0	< -8

gas-flow rate³⁴⁻³⁶ or by changing the reactor volume.^{14,15,17-19,36,37} Variation of the residence time by variation of the carrier gas-flow rate varies the concentration of the vapors, which could cause a change in the reaction pathways of the vapors and there with yields and compositions.^{15,22} Furthermore, in most setups the carrier gas-flow rate and, thus, residence time can only be varied to a limited extent to prevent defluidization or excessive entrainment of solids. In some studies, the reactor volume was varied (and so vapor residence time) by changing the fast pyrolysis reactor volume^{22,37} or by placing a second reactor in series.^{14,15,17,18} This last option makes it possible to decouple the fast pyrolysis—and vapor-phase temperature and was, therefore, used in this study together with a continuous vapor source.

Our Setup. The fluidized-bed reactor was identical to the one used in the pilot plant (section Pilot plant: analysis of in-bed char and minerals), however, in this setup no feed and withdrawal of sand was applied to ease operation. A flow sheet of the setup is given in Figure 2. The whole setup including the fluidized-bed reactor and tubular reactor will further be referred to as “FB+T-reactor” which is an abbreviation for “fluidized bed + tubular”-reactor.

Lignocel 9 was fed via a screw into the fluidized sand bed (at a height of $\sim 80\%$ of the total bed height). The fluidized-bed reactor was always operated at 500° C. The operating conditions of the standard run are summarized in Table 3. Preheated nitrogen gas ($3 \cdot U_{mf}$) was fed through a sintered plate. Because this setup was not operated continuously with respect to the solids phase, char built up in the course of an experiment (up to 25 vol % in 60 min). A custom made wire-mesh filter section (material purchased from Dinxperlo, wire weaving)⁹ was used to remove char from the gas/vapor stream. A schematic representation of this filter section is shown in the upper side in Figure 2. The first filter had a pore size of 9 μ m and was placed just above the fluidized bed. A second filter with a pore size of 5 μ m, length of 8.5 cm and a diameter of 2.2 cm was placed at the fluidized-bed reactor exit (just before tubular reactor inlet). The solids content of the pyrolysis oil obtained without the use of the tubular reactor was always below the detection limit (<0.002 wt %) indicating that a virtually solids-free gas/vapor stream was generated by using the filters. The temperature of the vapors leaving the fluid bed was controlled by heat tracing wrapped around the pipe (ID: 0.75 cm) connecting the fluidized bed and tubular reactor. The average deviation of the entrance tubular reactor temperature from the set-point of the tubular reactor (400, 500 or 550° C) was 6° C.

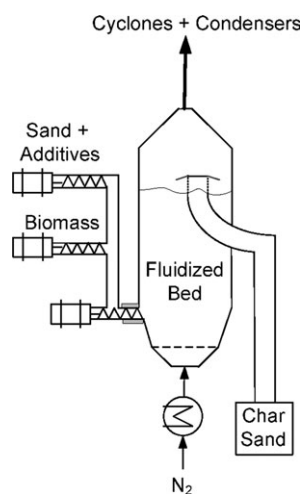


Figure 1. Char/mineral holdup regulation system pilot plant.

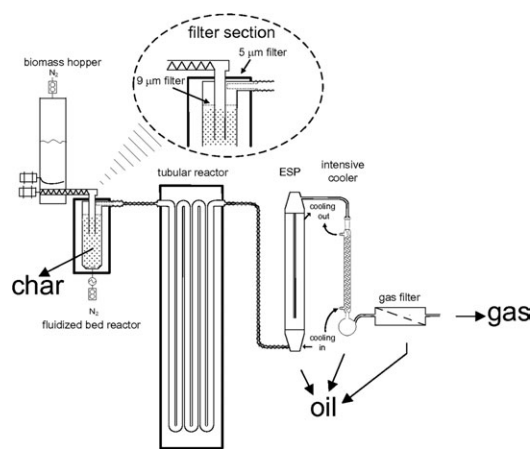


Figure 2. Fluidized bed and tubular reactor placed in series (FB+T-reactor).

Table 4. Used to Analyze Pyrolysis Oil

Compound	Technique	Analyzed Oil	Ref.
Water	Karl-Fischer titration	All condensers	9
C,H,O,N	Elemental Analyzer	ESP FB+T-reactor	9
Pyrolytic Lignin (water insolubles)	Cold water ($\sim 0^{\circ}\text{C}$) precipitation	ESP FB+T-reactor	24,25
Solids Content	Gravimetry	ESP FB+T-reactor	26
M_w -distribution (> 100 g/mol)	SEC (RID-detector)	ESP FB+T-reactor Spry column pilot plant	27
Aromatic and unsaturated conjugated compounds	SEC, ratio UV and RID detector	ESP FB+T-reactor	27
Volatile compounds	GC/MS (FID and MS detector)*	ESP FB+T-reactor	28

*Analysis carried out by vTI (Germany)

The residence time of the pyrolysis vapors inside the fluidized-bed reactor itself was approximately 1.5 s.

In the tubular reactor system (placed after the pyrolysis unit) four different tubular reactors constructed of AISI 316 steel with lengths of 1, 2.5, 8 and 11 m, and an inner diameter of 3 cm were used. The additional vapor-phase residence time in these tubular reactors varied from 1 till 15 s, and its temperature was maintained at 400, 500 or 550°C. The temperature of the tubular reactor was regulated within 3°C by an electrical oven in which four heating zones could be controlled independently. The Reynolds number of the gaseous stream was in the range of 275 (550°C) – 385 (400°C), indicating that the flow was laminar. The Peclet number as calculated from $\langle v \rangle L/D_{ax}$ varied from about 20 (400°C, 1 m) till 260 (550°C/11 m), indicating near plug flow behavior.

The vapor stream leaving the tubular reactor was condensed in a custom made jacketed electrostatic precipitator (ESP tube ID: 6.2 cm/L: 44 cm) operated at 17– 21 kV. The temperature of the outgoing stream of this condenser was kept below 24°C by pumping tap water through the annular space of the ESP. To the best of our knowledge, we are the first who are using a cooled ESP as main condenser directly after the reactor. Hereafter, the remaining uncondensed gas/vapor stream was sent to an intensive cooler ($T < -8^{\circ}\text{C}$), and a gas filter placed in series. About 97 wt % of the condensed organics was captured in the ESP, 2.7 wt % in the intensive cooler and 0.3 wt % in the gas filter. The oil was stored in a freezer at -20°C to prevent aging reactions.³⁸

Product collection and analysis

Biomass. The elemental composition (Fisons Instruments 1108 CHNS-O), ash content (NPR-CEN/TS 15403–550°C), water content (drying in an oven at 105°C for 24 h³¹), and alkali/alkaline content (measured at vTI, Germany using

ICP-OES) of the biomass feeds are reported in Table 1. The amount of dry ash free (daf) biomass fed during a run was determined by adjusting the mass difference of the biomass hopper before and after an experiment for the water and ash content of the feed.

Gases. The procedure to determine the gas yield in the pilot plant reactor (section Pilot plant: analysis of in-bed char and minerals) is described in detail in an earlier publication.³¹ In the FB+T-reactor the nitrogen flow rate was set by a calibrated mass-flow controller (Brooks). Gas samples were taken every 10 min. These samples were analyzed in a gas chromatograph for H_2 , CH_4 , CO , CO_2 , C_2H_4 , C_2H_6 , C_3H_6 , C_3H_8 (Varian Micro GC CP-4900 with two analytical columns, 10 m Molsieve 5A and 10 m PPQ, using helium as carrier gas). The sum of C_2H_4 , C_2H_6 , C_3H_6 and C_3H_8 will further be referred to as C_{2+} . The total outgoing mass of an individual gaseous compound was calculated by multiplying its gaseous mole fraction by the total flow rate ($\phi_{v,\text{total}} = \phi_{v,\text{N}_2}^*(100/(100 - \sum \text{mol \% gases})))$, and molecular mass of that compound and, subsequently, integrating over time. The total gas yield on dry ash-free basis was calculated by summing the yields of the individual gas compounds and dividing this value by the amount of daf biomass fed during the run.

Pyrolysis Oil. The procedure to determine the oil yield in the pilot plant reactor (section Pilot plant: analysis of in-bed char and minerals) is described in detail in an earlier publication.³¹ For the FB+T-reactor the daf oil yield was determined by (a) summing the weight of oil collected in the ESP, intensive cooler and filter, (b) subtracting the amount of water which was already present in the feed, and (c) dividing the resulting weight by the amount of daf biomass fed during the run. The composition of the oil was determined by various techniques as listed in Table 4.

Char. The procedure to determine the char yield in the pilot plant reactor (section Pilot plant: analysis of in-bed char and minerals) is described in detail in an earlier publication.³¹ The char yield (daf) for the FB+T-reactor was determined by dividing the mass of char collected inside the bed and on the filters minus the amount of minerals present in the feedstock by the amount of daf biomass fed during the run. So, it was assumed that all minerals present inside the feedstock end up in the char phase. It should be noted that the char yield determined as described earlier is independent of the conditions in the tubular reactor that is placed after the pyrolyzer.

Heterogeneous Vapor-Phase Reactions

To study the influence of the contact of vapors with char and minerals a series of experiments (Table 2) was carried out using the pilot plant. In these experiments the char content and mineral (Na + K) content was varied. The oil (organics and water), char and gas yields are plotted in

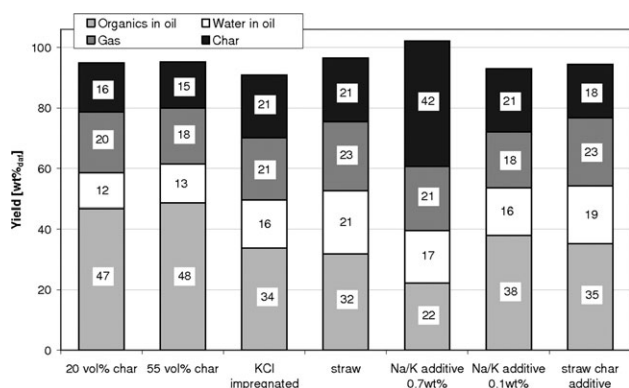


Figure 3. Yields, experimental conditions reported in Table 2

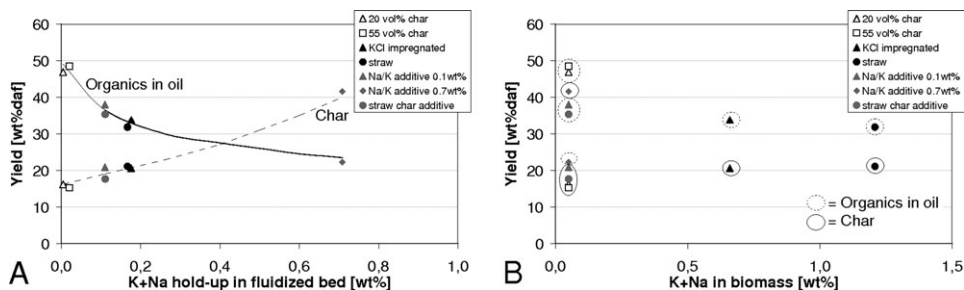


Figure 4. Organic yield as function of the wt % of K + Na inside the fluidized bed and biomass particles.

Figure 3. The corresponding molecular-weight distributions of the oils can be found in Figure 5. The organic and char yield as function of the K+Na holdup for all experiments is plotted in Figure 4. It should be kept in mind that the char and mineral holdup (vol % and wt %) are expressed on total solid (char + sand + minerals) basis (see section 2.2).

Effect of char holdup: feedstock (500 ppm Na+K) derived char

In the pilot plant, two experiments using Lngnocel 9 (with only 500 ppm Na + K) as feedstock and a char holdup in the fluidized bed of 20 and 55 vol % were carried out. The extent of possible vapor-char interactions was expected to increase with rising volumetric char holdup. However, similar gas, oil and char yields were obtained, while also the amount of produced water was similar (Figure 3). No differences in molecular-weight distribution of the oil phase could be observed either (Figure 5A). The experiments were repeated at a lower temperature of 400°C, and higher temperature of 530°C (no data shown). Again no influence of char holdup was observed in those cases. Data obtained in the FB+T-reactor supported these observations. In this setup the char holdup linearly increased during the course of an experiment from 0 up to about 25 vol %. However, no change in the permanent gas concentration and composition was observed as function of the experimental progress/char holdup (Figure 6). These observations are in line with data

obtained by Shen et al.¹⁰ who performed similar experiments, but contradictory to earlier observations of Boroson et al.¹⁴ and Ahuja et al.²³ who did observe an effect of char. Our data indicate that vapor-char interactions from an (almost) mineral free feedstock do not influence the product yields in our pilot plant noticeably.

Effect K + Na in feedstock

Two experiments using different feedstock's high in K/Na content were carried out. One experiment was carried out in the pilot plant using Lignocel 9 impregnated with KCl. Because impregnation is an artificial way of increasing the mineral content of the feed, straw was also used as feed (Table 1). In both cases, the liquid organic yield dropped, the char and water yield increased (Figure 3), and the average molecular weight of the oil decreased (Figure 5B) compared to experiments carried out using untreated Lignocel 9. In addition, a slight increase in gas yield was observed for the "straw" experiment. Our data and the results reported in literature^{7,29,30} clearly show that the mineral content (especially Na and K) inside the biomass has an important effect on the product yields and product characteristics. Because the use of a mineral rich feedstock also results in the formation of mineral rich char, it is not clear whether the observed effects are due to differences in reactions (rate, pathway) inside the reacting biomass particle (internal) or because of

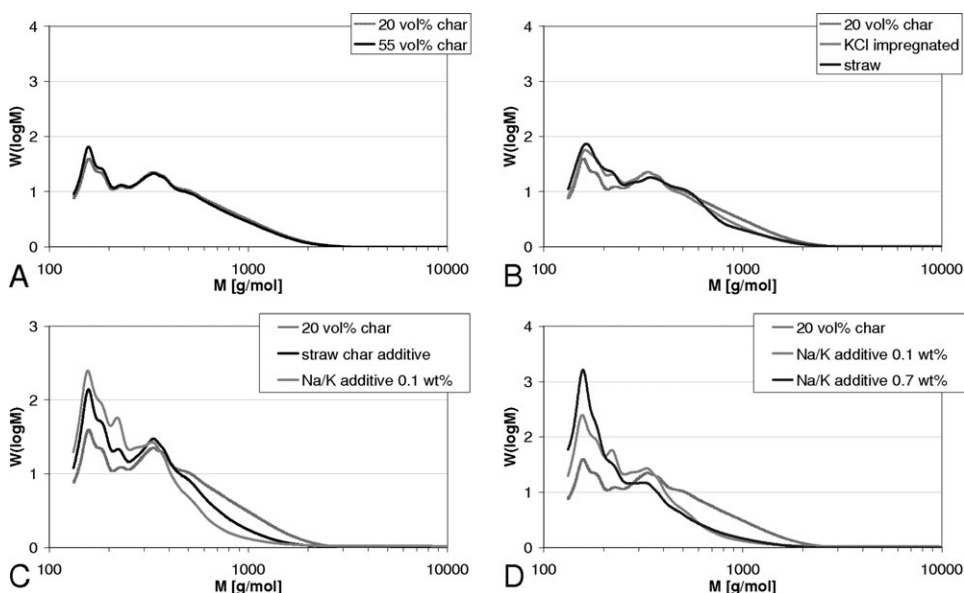


Figure 5. Mw-distribution of oils produced in pilot plant.

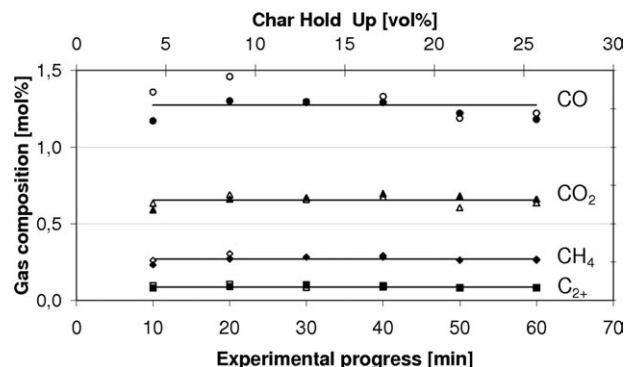


Figure 6. Gas composition as function of char-holdup/ time in FB+T reactor.

No tubular reactor installed, closed and open symbols denote two separate experiments.

reactions of produced vapors with already existing char (external). This will be discussed in the following sections.

Effect “external” K + Na on heterogeneous vapor-phase reactions

To reveal whether “external minerals” can affect the extent of vapor-phase reactions an additional series of experiments was carried out. In these experiments, untreated Lignocel 9 was used as feedstock; however, mineral rich additives were added to the feed of the fluidized bed. These additives were either Na/K salts (using two holdups, viz. 0.1 and 0.7 wt %), or a mineral rich char originating from straw (straw char holdup 25 vol %; Na/K holdup 0.1 wt %). The organic oil yield decreased, while the char and produced water yield increased as compared to the “20 vol % char” experiment (Figure 3). More gases were produced in the “straw char additive” experiment and the average molecular weight decreased for all experiments (Figure 3 and 5C,D), both phenomena suggesting some form of cracking. One experiment was carried out with a much larger amount of added salts to the bed: “Na/K additive 0.7 wt %”. The results in Figure 3 show that less oil and more gasses, water and char were produced, and the average molecular weight of the oil was decreased in comparison with the experiment using 0.1 wt % Na/K. The yield of char even doubled to 42 wt %.

Our results clearly show that after leaving the biomass matrix vapors react on the (internal) surface of particles with inorganic matter to form additional char, water and an oil with a lower molecular weight. Heterogeneous vapor-phase charring/polymerization reactions were more important than cracking reactions of vapors to gas.

Na+K in biomass vs. Na+K in the reactor (FB)

A decline in organic yield and an increase in char yield were observed with increasing total Na + K holdup inside the fluidized-bed reactor (Figure 4A). However, no relationship could be observed between the amount of Na + K present inside the biomass feedstock and the yields of organics and char (Figure 4B). From these experimental data it can be concluded that in the studied range (Tables 2 and 3) external interactions between the vapors and Na/K rich solids do play a more significant role than the interactions between Na/K and the (decomposing) biomass (internal). However, several TGA (heating rate 10 °C/min)^{30,39} and Py-

GC/MS^{40,41} (heating rate > 2000°C/s) studies report that minerals like K and Na have an effect on the decomposition “weight loss” reactions of biomass, cellulose and hemicellulose. When adding for instance KOH to pine wood the temperature at which the highest weight loss rate was observed reduced significantly from 353 to 275°C.³⁹ Although minerals influence the initial decomposition reactions this could not be established in this study because of the predominance of external interactions between the vapors and Na/K rich solids. More research is necessary to elucidate the effect of minerals on a (decomposing) biomass particle in the absence of vapor-particle interactions.

Concluding remarks

The results clearly show that char itself, viz. the organic C,H and O atoms in it, appear *not* to be catalytically active inside the fluidized-bed reactor. However, the presence of minerals (Na/K)—either in the biomass matrix (native or impregnated) or external (as salt or in char), does influence the fast pyrolysis process. In our experiments external interactions between the vapors and Na/K rich solids did play a more significant role than internal interactions between Na/K and the (decomposing) biomass. Heterogeneous vapor-phase charring/polymerization reactions were more important than cracking reactions of vapors to gas. From these results it is evident that the contact between minerals and vapors needs to be minimized to be able to obtain high-oil yields.

Homogeneous Vapor-Phase Reactions

Homogeneous vapor-phase reactions from char-free pyrolysis vapors were studied in the FB+T reactor system. It is important to realize that the pyrolysis vapors that were introduced in the tubular reactor were already exposed for ~1.5 s to the temperature in the fluidized-bed reactor (500°C). The gas and oil yield as function of the tubular reactor conditions and the corresponding char yield in the fluid bed are shown in Figure 7. The mass balance closure is plotted in the same figure, and is around 90 wt % for all experiments. This gap is expected to be related to the loss of some volatile compounds which might be stripped from the condensation system due to the high $\Phi_{v,N_2}/\Phi_{m,biomass}$ ratio applied (Table 3). Three identical runs were carried using the fluidized-bed reactor alone to get an indication of the experimental error and are plotted as reference (designated as “0.0 s”). The product

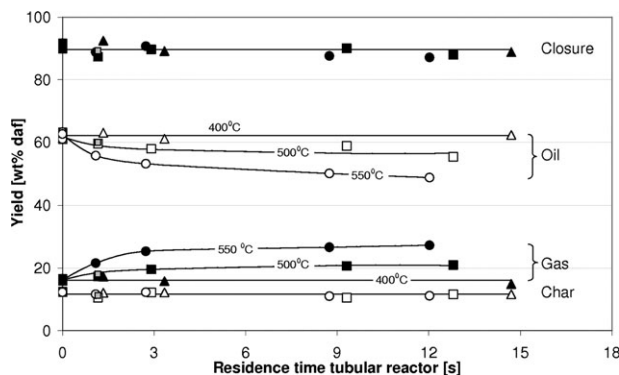


Figure 7. Yields at different tubular reactor temperatures and residence times, residence time in fluid bed ~1.5 s (▲ △ = 400°C, ■ □ = 500°C, ● ○ = 550°C, = steel wool 500°C).

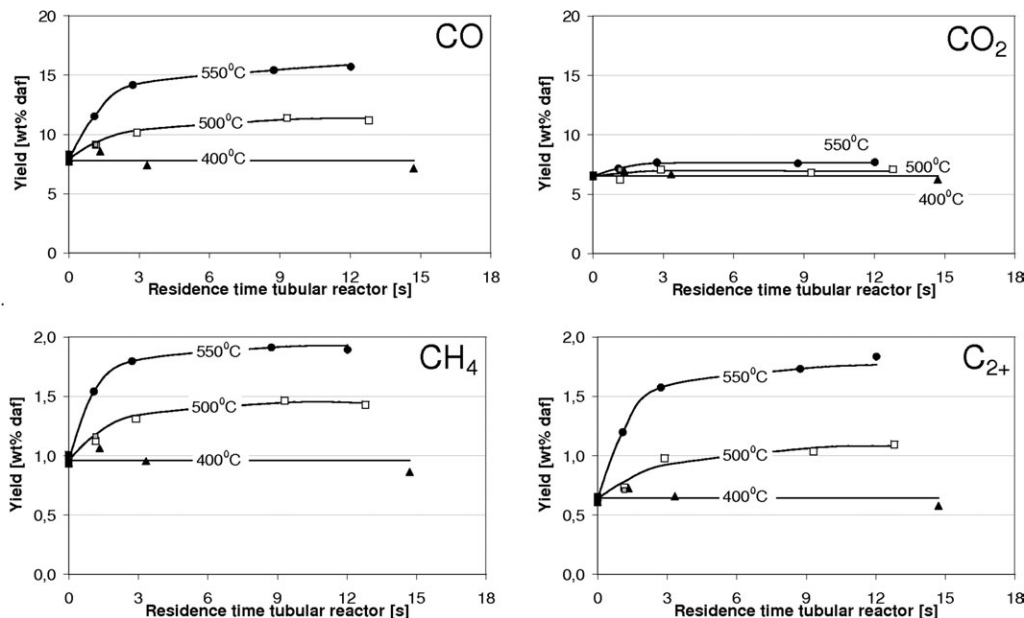


Figure 8. Gas yields at different tubular temperatures and residence times (triangle = 400°C, square = 500°C, circle = 550°C, = steel wool 500°C).

yields and oil composition show good reproducibility (Figures 7–13).

Heterogeneous reactions on reactor wall

In the downstream tubular reactor, heterogeneous reactions of vapors in contact with the (hot) stainless steel reactor wall cannot be excluded. Minor char deposits were visually observed on the tubular reactor wall. This is in accordance with previous results which showed that some char can be formed on various surfaces from a solids-free vapor stream.⁹ An estimation of the amount of char deposited on the tubular reactor wall was made after finishing all experiments. The 1 m tubular reactor was weighed, cleaned (by burning) and, subsequently, reweighed. Assuming the weight difference to be caused by only deposited char, this amount appeared to be only 0.1 wt %_{daf} (average over all runs with 1 m tubular reactor). To study the influence of a fivefold larger steel area on the vapor-phase reactions the 1 m tubular reactor was filled with steel wool. The results were similar to these obtained without steel wool (Figures 7–10). Assuming that the increase in mass of the steel wool afterward was due to char formation, this was again a negligible percentage (+0.05 wt %_{daf}). It can thus be concluded that the possible catalytic effect of the steel tubular reactor wall is insignificant.

Yields: oil, gas, char

The measured char yield in the fluid bed should of course be independent on the process conditions in the tubular reactor placed after the fluid bed. This was indeed the case; about 12 wt %_{daf} of char yield was obtained in all experiments. Char formation inside the tubular reactor could only be quantified indirectly. No solids were detected inside the pyrolysis oil (<0.002 wt %) and, as already shown in the section Heterogeneous reactions on reactor wall, an insignificant amount of char was deposited on the section Heterogeneous reactions on reactor wall. These results indicate that for the process conditions applied negligible amounts of char were formed from homogeneous vapor-phase reactions.

The oil and organic yield did follow the same trend since the water production was constant for all tubular reactor conditions (see section 4.3). The oil and gas yield remained constant and were independent on residence time if the tubular reactor was operated at 400°C. At 500°C and in the first 5 s, a slight decrease in oil yield (~5 wt %_{daf}), and a similar increase in gas yield was observed. The oil and gas yield remained nearly constant hereafter. At 550°C, the oil yield decreased and gas yield increased with slightly more than 10 wt %_{daf}. The yields appeared to be almost completely stabilized with time up to 12 s. In literature it is regularly reported that the oil yield decreases continuously with increasing residence time (studied up to 3.5 s^{19,20,42}). Our results show that this trend cannot be extrapolated to higher residence times. Boroson et al.¹⁵ postulated the existence of such a temperature-dependent asymptote based on a measured constant oil yield at 800°C for residence times between 1.6 and 2.0 s. Although their maximum residence time of 2 s was not long enough to observe the asymptotes at typical pyrolysis temperatures, our data shows that their postulation is indeed correct for temperatures between 400 and 550°C. Graham et al.¹⁶ studied the vapor-phase reactions during the pyrolysis of cellulose and also in that case asymptotic oil yields were obtained, but much faster than Boroson observed: within 1 s for temperatures in the range of 650–800°C. These results show that a temperature-dependent asymptote is present provided that long enough vapor residence times are applied. With increasing temperature an increasing part of the pyrolysis vapors can crack to gases via homogeneous vapor-phase reactions.

The effect of the vapor residence time and temperature on the yields of the individual gas compounds (CO, CO₂, CH₄, C₂₊) is shown in Figure 8. Based on thermodynamic calculations (RGibbs reactor in Aspen Plus) and experimental data of Lanza et al.²² water-gas shift and methane reforming reactions are not expected to play a significant role in the temperature range used (400–550°C). Therefore, the change in especially CO₂, CO, H₂O, CH₄ and H₂ must originate

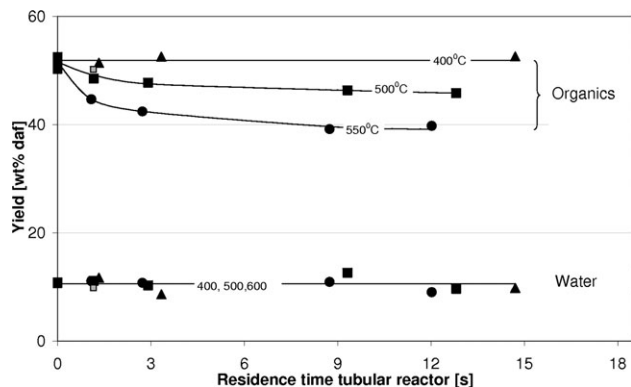


Figure 9. Yields of organics and produced water as a function of tubular temperature and residence time (triangle = 400 °C, square = 500 °C, circle = 550 °C, = steel wool 500 °C).

directly from pyrolysis vapor reactions. According to Figure 7, no change in gas yield was observed if the tubular reactor was operated at 400°C, and also the gas yield of the individual compounds remained constant. The gas yields for all individual compounds increased with reactor severity for temperatures above 500°C. Especially the yield of CO was increasing with increasing reactor severity (~70% of additional formed gases on weight basis), while the yield of CO₂ increased only marginally (~10% of the additional formed gases on weight basis). The C₂₊ yield showed the largest relative increase, almost tripling at 550°C/12 s. The CH₄ yield doubled under those conditions. The increase of the CO/CO₂ ratio with the extent of vapor phase reactions (i.e., temperature, residence time) is in line with previous results obtained using batch wise operated pyrolysis reactors with subsequent tubular reactor using wood^{15,17,18} and model compounds^{43–45} as feedstock.

Although the pyrolysis oil yields do not (400°C) or marginally (500°C) change as a function of the residence time in the tubular reactor, it is not clear whether changes in composition by vapor to vapor reactions occur for these experiments. Additional analytical techniques were used to study these possible changes.

Water production

According to literature, several dehydration reactions of pyrolysis vapors can occur, for example during the formation of isoeugenol,⁴³ furans,^{44–46} ketenes⁴⁴ (which can rehydrate to form acids), and several monosaccharides⁴⁹ and anhydro-sugars.⁴⁷ Condensation reactions of pyrolysis oil are known to take place even at room temperature.⁴⁷ Possibly, water can also be formed via (bimolecular) condensation reactions inside the vapor phase. However, no differences in water production could be observed between the various experiments (Figure 9) indicating that dehydrations reactions occurred mainly inside the fluidized-bed reactor ($\tau \sim 1.5$ s). An average water production value of 10.5 wt % was measured, with a standard deviation of 1.0 wt %.

Elemental composition of oil (organics)

Considering that the water and char production were independent of the conditions in the tubular reactor, the change in elemental composition of the oil should directly be related to the change in elemental composition and yield of the gas

phase. For the most severe conditions—11 m tube, 550°C—a calculated change in elemental oil composition of only +1.1, + 0.3 and –1.4 wt % for C, H and O would be expected. In line with these expected small changes, the measured elemental composition appeared to be independent on the process conditions in the tubular reactor and similar to the one of the oil obtained directly after the fluidized-bed reactor: C = 57 \pm 0.8 (STDEV), H = 6 \pm 0.9, and O = 36 \pm 0.2 wt %_{daf}.

Molecular-weight distribution

The molecular-weight distributions of the oils produced in the shortest (1 m, $\tau = 1$ s), and longest (11 m, $\tau = 12$ –15 s) tubular reactor operated at 400, 500 and 550°C are plotted in Figure 10. The oil produced in the fluidized-bed reactor alone is plotted as reference in the same figure (0.0 s). The area under the SEC curves is normalized to 1, so the peak heights/area are not related to the actual yield of a molecular-weight fraction, but to (a certain extent to²⁷) the relative presence of it inside the oil.

A small decrease in average molecular weight with respect to the reference oil was observed for the experiments carried out in the tubular reactor operated at 400°C. It was shown before (Figure 8) that no additional gases were formed at this temperature, so vapor molecules are likely to have rearranged and cracked to smaller ones that end up in the oil phase upon condensation.

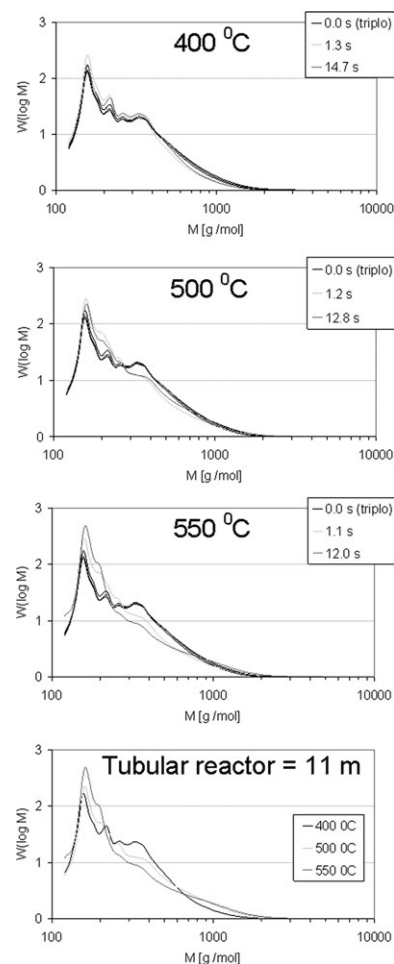


Figure 10. Mw-distribution of pyrolysis oil.

Time gives residence time in tubular reactor system.

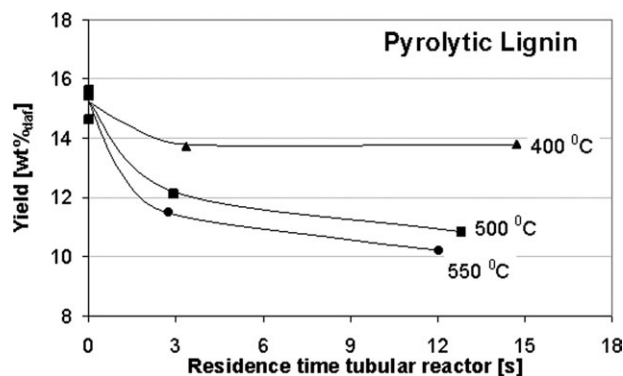


Figure 11. Pyrolytic lignin (water-insolubles).

A significant reduction in the peak intensity around 200–350 g/mol was observed when the tubular reaction system was operated at 500 °C. The center plateau at 200–350 g/mol disappeared completely at 550 °C, and a vapor-phase residence time of 12.0 s indicating cracking reactions. The occurrence of cracking reactions is supported by the aforementioned increase in gas yield at the expense of oil yield (section Yields: oil, gas, char). The oil produced with the tubular reactor operated at 500 and 550 °C did contain relatively more compounds with higher-molecular weight (>1000 g/mol) than the reference oil and the oil produced in the FB+T at 400 °C. It cannot be unambiguously concluded whether these compounds are really formed by polymerization reactions or if it is only a relative increase which can be explained by the disappearance of low-molecular-weight compounds due to the formation of gases. Because no increase in pyrolytic lignin content (see next paragraph) and no noticeable increase in water production (condensation reactions) was observed, the second explanation is favored.

Pyrolytic lignin content

In Figure 11 the pyrolytic lignin yield (water-insolubles) is plotted as function of the vapor-phase residence time. Pyrolytic lignin is known to account (partly) for the high-molecular-weight compounds present in pyrolysis oil.¹¹ The pyrolytic lignin content dropped at 400 °C which is in line with the M_w -distribution results. This supports the aforementioned finding that vapor molecules do crack at 400 °C to smaller molecules, although no oil yield changes were observed. The pyrolytic lignin yield dropped further upon increasing the tubular reactor temperature to 500 and 550 °C, which is in line with the observed decline in average molecular weight of the oils. These results and the results on the M_w -distribution of the oils suggest that cracking reactions were dominant over polymerization reactions in the studied range (400–550 °C/1–15 s).

Aromatic and conjugated (AC) compounds

The $\int UVdv/\int RIDdv$ ratio which is associated with the relative content of the aromatic and conjugated (AC) compounds in the oil²⁷ is plotted as function of the tubular reactor severity in Figure 12. The $\int UVdv/\int RIDdv$ ratio for the oil remained constant for the experiments carried out at 400 °C. The amount of AC compounds appeared to increase with increasing tubular reactor severity. In literature it is regularly reported that pyrolysis oil produced at higher temperatures contains more aromatics.^{19,36,48} Aromatization reactions are reported to take place at higher temperatures.⁴⁸ A second

explanation opposite to the formation of AC compounds is that non AC compounds might be gasified which should be accompanied by an oil yield decrease and a relative higher abundance of AC compounds. Although it is unknown if a linear relation exist between the $\int UVdv/\int RIDdv$ ratio and the concentration of AC compounds, the yield corrected $\int UVdv/\int RIDdv$ ratio's are plotted as well in Figure 12 (open symbols). The yield corrected $\int UVdv/\int RIDdv$ ratio was independent of the tubular reactor severity. This suggests that higher concentrations of aromatics as often observed in the oil with an increase in pyrolysis severity does not necessarily imply the net formation of aromatics, but can also be explained by the net disappearance of the nonaromatic fraction from the oil.

GC/MS: volatile compounds

An indication of the fraction of volatile compounds in the pyrolysis oil was obtained by using GC/MS. The total yield of volatile compounds, levoglucosan and the yield of four lumped groups (nonaromatic aldehydes, pyrans, guaiacols, lignin derived phenols) are plotted in Figure 13 as function of the tubular reactor temperature (400, 500, 550 °C), and residence time (0–15 s). The detected and quantified compounds in these four groups are listed in Table 5.

At 400 °C, the sum of total GC/MS detectables (~volatiles) increased with residence time, while no oil yield changes were observed at this temperature. This shows that also at 400 °C vapor to vapor reaction occur and heavier molecules are likely to be cracked to more volatile ones. This is in line with the SEC analysis result and the pyrolytic lignin content (see sections Molecular weight distribution and Pyrolytic lignin content). At higher temperatures (500 and 550 °C), the yield of volatile compounds decreased with residence time, but also an increase in gas yield was observed for these experiments. Summing the gas and volatile yield showed that its value increased with residence time for all temperatures. So, overall, heavier molecules were cracked to smaller ones (either volatiles or gases) for all temperatures. From this we conclude that the overall formation of GC/MS detectable volatile compounds from heavier vapor components is slower than the overall cracking of GC/MS detectable volatiles to gases at 500 and 550 °C.

Nonaromatic aldehydes are reported to mainly originate from pyrolysis of hemicellulose and cellulose.^{44,45} The yield of nonaromatic aldehydes initially (up to ~3 s) increased for

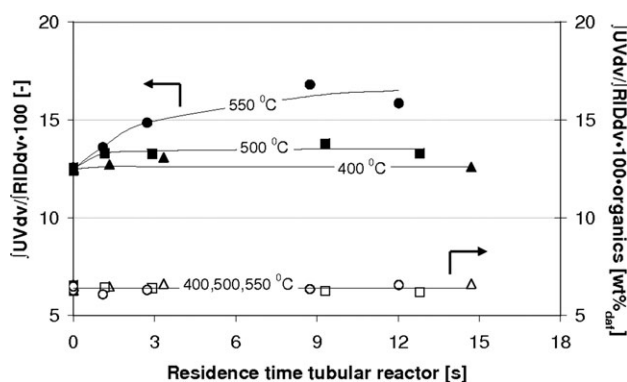


Figure 12. $\int UVdv/\int RIDdv$ ratio for pyrolysis oil (associated with aromatic and conjugated compounds).

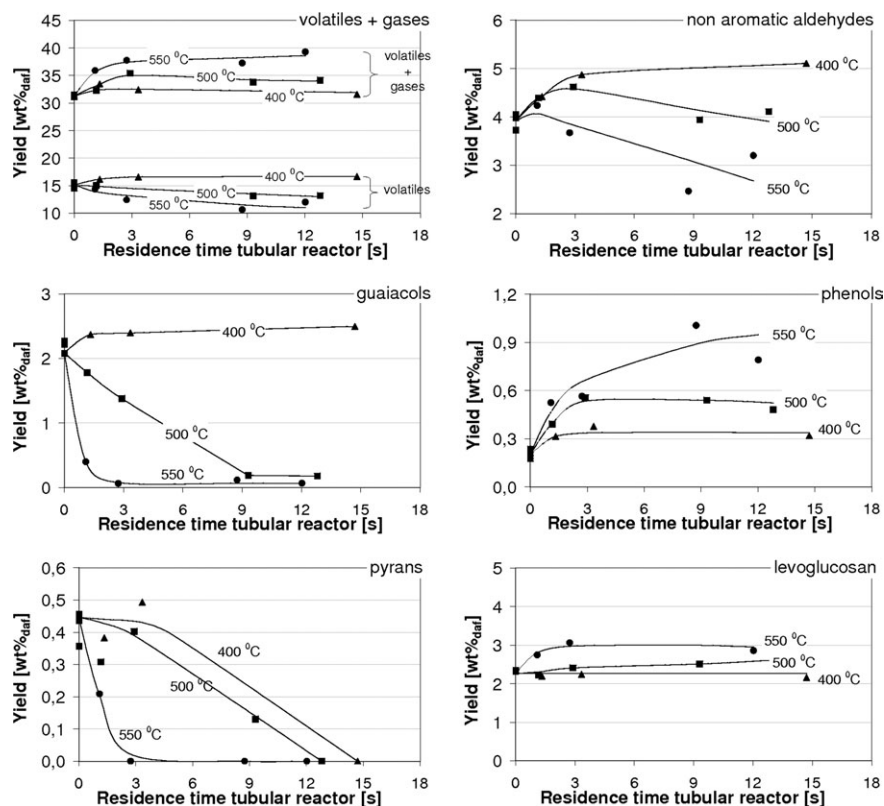


Figure 13. Yields of GC/MS detectable volatile compounds (denoted as volatiles) in FB+T reactor (triangle = 400°C, square = 500°C, circle = 550°C).

all temperatures after which a decline was observed for the two highest temperatures only. Aldehydes appear to be formed from heavier molecules during pyrolysis vapor-phase reactions even at temperatures as low as 400°C for which no oil yield changes were observed. Since an increase in CO yield was observed only at 500 and 550°C, and aldehyde type of compounds are reported to be cracked to CO,^{44,45} it is likely that the decline in aldehyde yield can be explained by subsequent decarbonylation reactions. Overall, part of the heavier hydrocarbons seem to be converted to nonaromatic aldehydes (>400°C) and CO (>500°C).

Pyrans originating from the degradation of several (poly)saccharides⁴⁹ appeared not to be stable in the range of 400–550°C as is shown in Figure 13. These results proof again that at 400°C internal rearrangement reactions took place although no changes in yields were observed.

Levoglucosan is one of the most abundant products in pyrolysis oil and originate primarily from cellulose.^{44,49,50} Figure 13 shows that the levoglucosan yield was constant at 400°C. At higher temperatures, the small increase in levoglu-

cosan yield might be explained by further cracking of cellulose decomposition products (e.g., cellobiose). In literature several reactions schemes of levoglucosan are reported. Cracking reactions of levoglucosan to lower molecular weight products like furans and aldehydes,^{44,50} but also polymerization reactions of levoglucosan to form polysaccharides⁵⁰ are included in those schemes. Our results did show that such kind of reactions do not take place inside a homogeneous vapor phase at temperatures between 400 and 550°C.

In literature it is reported that softwood lignins typically degrade to guaiacol-type of compounds⁵¹ and guaiacols are reported to be converted to phenols and catechols.^{36,43,51} The methoxy group (–OCH₃) was suggested to be an important source for the formation of the small volatile species (CO, CO₂ and CH₄).⁴³ 2.3 wt %_{daf} of guaiacols were detected inside the pyrolysis oil collected just after the fluidized-bed reactor. Although at 400°C guaiacols appeared to be stable, they disappeared almost completely with increasing severity in the tubular reactor. An increase in gas yield and lignin

Table 5. Lumped Classes of Volatile Pyrolysis Liquid Compounds, Quantified by GC/MS

Class	Quantified compounds
Non aromatic aldehydes	hydroxy-acetaldehyde, 3-hydroxy-Propionaldehyde, crotonaldehyde, butandial, 2-methyl-propanal
Pyrans	3-hydroxy-5,6-dihydro- (4H)-Pyran-4-one
Phenols	phenol, cresol (o,m,p), dimethyl-phenol (2,5 and 2,6), trimethyl-phenol (2,3,6 and 2,4,6), ethyl phenol (2 and 3 and 4), trimethyl-derivative of phenol, (2,3,4- of 2,4,5-), 2-hydroxy-benzaldehyde, 2-hydroxy-4-methylbenzaldehyde
Guaiacols	guaiacol, 4-methyl-guaiacol, 4-ethyl-guaiacol, 4-vinyl-guaiacol, 4-allyl-guaiacol, (eugenol), 4-propenyl-(cis/trans)-guaiacol, (=isoeugenol), vanillin, homovanillin, coniferyl alcohol, acetoguaiacone, propioguaiacone, guaiacyl acetone, coniferylaldehyde, 4-hydroxy-3-methoxy-benzoic acid methyl ester

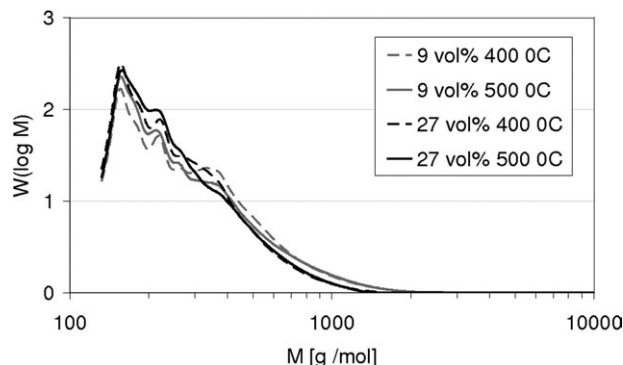


Figure 14. Effect of vapor/gas concentration on the Mw-distributions of the oils.

derived phenols was observed simultaneously at 500 and 550°C which is expected based on the reaction pathway proposed in literature.

Effect concentration on polymerization reactions

The results described in the sections Yields: oil, gas, char and GC/MS: volatile compounds suggest that cracking reactions were dominant over polymerization reactions in the studied range ($C_{\text{gases+vapors}} = 9 \text{ vol\%}$ 400–550 °C/1–15 s). No increase in char yield, water production (linked to condensation reactions), pyrolytic lignin content and absolute molecular weight was observed which are all indicators for the occurrence of polymerization reactions. It should be emphasized that nitrogen diluted pyrolysis vapor streams were used (because of the fluid-bed technology) and the concentration of the vapors is, thus, low. Polymerization reactions are expected to be bimolecular and its rate thus expected to be concentration dependent. Since in literature no data are reported about the effect of pyrolysis vapor concentration on homogeneous vapor-phase reactions some preliminary tests were carried out with a three times higher concentration ($C_{\text{gases+vapors}} = 27 \text{ vol\%}$, $\tau = 3 \text{ s}$, $T = 400$ and 500°C). The higher concentration was reached by reducing the reactor diameter (ID 5.5 cm vs. 10 cm), and by reducing the minimum fluidization velocity ($d_{p,\text{sand}} = 200 \mu\text{m}$ vs. $d_{p,\text{sand}} = 200\text{--}300 \mu\text{m}$). No decrease in oil yield was observed for the 27 vol % compared to the standard runs with a vapor and gas concentration of 9 vol %. The molecular-weight distributions of the resulting oils are shown in Figure 14. No additional polymerizations reactions appeared to occur for the more concentrated pyrolysis vapor stream (27 vol %). So, the findings reported in this study are expected to be valid for more concentrated vapor streams as well.

Kinetics, Mechanism and Modeling of Vapor-Phase Reactions

The degradation of biomass is traditionally described via three parallel first-order reactions to gas, oil and char.^{52,53} More comprehensive pyrolysis reaction models include homogeneous vapor-phase reactions. The background of some of these models is discussed below in relation to the results obtained in this study.

Homogeneous vapor to gas reactions are often modeled using simple first-order kinetics.^{20,21,42} Baumlin et al.²⁰ constructed an Arrhenius plot of the first-order rate constants of vapor to gas as reported in literature. The calculated Arrhe-

nius constants for our own results (500–550°C, first 2 s, isothermal plug flow model $k_0 = 1.8 \cdot 10^5 \text{ s}^{-1}$, $E_a = 9.7 \cdot 10^4 \text{ J/mol}$) lie within the range of literature data. However, the spread in reported k values was large with differences up to a factor 15. This spread in reported k values was attributed to the difference in feedstocks (type, particle size), reactor (type, heating rate, reactor material) and calculation procedures.^{15,20} Although the aforementioned model can predict the trend for short vapor residence times, it cannot predict the asymptotes in oil yield we did observe at prolonged vapor residence times (Figure 7). These asymptotes can be predicted if not the actual oil yield, but the difference between the actual and the stable oil yield (i.e., minimum oil yield at a specific T) is used in the kinetic expression. However, such models appear to underpredict the conversions at short vapor phase residence times¹⁵ probably due to the presence of vapors with different reactivities.

Some researchers^{15,17–19} extended the concept of first-order oil vapor to gas reactions by introducing several parallel first-order vapor to gas-cracking reactions. Boroson et al.¹⁵ and Stiles et al.¹⁹ assumed an infinite number of reactions to occur (distributed activation energy model) while Rath et al.^{17,18} divided the pyrolysis vapors into three reactive fractions. Such models are able to predict the asymptotes as observed in this study, but do not take into account any type of vapor to vapor reactions which were proven to occur in this study (see section Yields: oil, gas, char). Antal³² took those types of reactions into account in his model by including two parallel first-order vapor reactions: one to permanent gases and the other one to stable vapors. Missing in Antal's model is a distinction between the reactivity of the different type of vapors originating from the biomass matrix (cellulose, hemicellulose and lignin).

Combination of the work of Boroson et al.¹⁵ and Antal³² would yield a model that represents the homogeneous vapor-phase reactions better. However, our work has shown that heterogeneous vapor reactions have a large influence on oil yield and composition as well. So far, and to our knowledge little to nothing has been done on the description and modeling of these heterogeneous vapor-phase reactions.

The systematic approach dealing with the heterogeneous and homogeneous vapor phase reactions as carried out in this study cannot only help to obtain a better understanding of the complex pyrolysis system but also elucidate the feasibility of modeling such system reliably. We believe that a *generic* mathematical description of the pyrolysis reactions either leads to a dangerous oversimplification or to a model with far too many (unknown) fit parameters. To our opinion, and at this point in time, simple models based on measurable parameters supported by good understanding of the actual phenomena taking place (decomposition and vapor-phase reactions) allows for the most reliable prediction/extrapolation of the performance just outside the measured area for which the models were derived.

Engineering Viewpoint

Several reactor types for fast pyrolysis processes have been and are being developed like (1) bubbling-fluidized bed, (2) transported bed, (3) circulating fluidized bed, (4) ablative pyrolysis, (5) auger, and (6) vacuum pyrolysis. Their advantages and disadvantages are described extensively in literature.^{1,5,7,13,54} Three statements which are important

from an engineering point of view are formulated based on our experimental results.

1 *It is not necessary to remove ash poor char (C,H,O) directly from the hot pyrolysis vapor stream.* No changes in yields and oil composition were observed as function of (mineral poor) char holdup (see section 3.1). Consequently it is not necessary to remove pure char (C,H,O) from the vapors. It should be noted that it is only possible to obtain an ash poor char from an ash poor feedstock. For this, either a clean feedstock like pine wood needs to be used or the minerals present in the biomass needs to be removed beforehand by a pretreatment step. Research did show that minerals can be removed by a relatively simple washing step using water.²⁹

2 *The contact time between vapors and minerals needs to be minimized.* Minerals, whether incorporated in the char matrix or not, appear to be detrimental for the pyrolysis oil yield. Contact between minerals and pyrolysis vapors should be avoided to prevent a decrease in oil yield. This can either be done by reducing the mineral concentration inside the reactor (for example prevent accumulation in continuous circulating processes), or by reducing the residence time of the vapors in the mineral rich part of the pyrolysis unit.

3 *Pyrolysis vapors (mineral poor) can be exposed to temperatures up to 400°C for long times.* At 400°C, homogeneous vapor-phase reactions do not influence the fast pyrolysis process in terms of oil yield. Rapid cooling of the vapors to ambient temperatures as typically reported in literature is, thus, not necessary.^{1,5–7} Although some extent of vapor to vapor cracking was observed at 400°C, this was not accompanied by changes in oil yield. It should be noted that the pyrolysis vapors were produced at a typical pyrolysis temperature of 500°C, and statement three may not be valid for lower pyrolysis temperatures.

Conclusions

Heterogeneous and homogeneous reactions of pyrolysis vapors from pine wood were studied using, respectively a fluidized-bed reactor (500°C, ~0.8 kg/h), and a fluidized-bed reactor (500°C, 0.15 kg/h) connected to a tubular reactor (1–15 s, 400–550°C).

Char itself, viz. the organic C, H and O atoms, appeared *not* to be catalytically active inside the fluidized-bed reactor. However, the presence of minerals (Na/K)—either in the biomass matrix (native or impregnated) or external (as salt or in char), does influence the fast pyrolysis process. In our experiments external interactions between the vapors and Na/K rich solids did play a more significant role than internal interactions between Na/K and the (decomposing) biomass. Heterogeneous vapor-phase charring/polymerization reactions were more important than cracking reactions of vapors to gas.

Pyrolysis vapors were also found to be reactive in the absence of minerals. With increasing temperature an increasing part of the pyrolysis vapors cracked to gases via homogeneous vapor-phase reactions. Our results show that a temperature-dependent oil yield asymptote is reached provided that long enough vapor residence times are applied (400°C: 62 wt %_{daf}, 500°C: 57, 550°C: 49). At a vapor temperature of 400°C, the oil and gas yield were independent on the residence time, but homogeneous vapor to vapor reactions were proven to occur. In the studied range (400–550°C, 1–15 s)

homogeneous cracking reactions were dominant over polymerization reactions. A decrease in average molecular weight, lignin content and an increase in gas yield (especially CO), and phenols (GC/MS) was observed which are all indicators for cracking reactions while no increase in char yield and water production was observed which are indicators for the occurrence of polymerization reactions. It was shown that literature models consider the homogeneous and heterogeneous vapor-phase reactions only to a limited extent.

Based on this work, three statements which are important from an engineering point of view could be formulated:

1. It is not necessary to remove ash poor char (C,H,O) directly from the hot pyrolysis vapor stream;
2. The contact time between vapors and minerals, whether or not incorporated in the char matrix, needs to be minimized;
3. Pyrolysis vapors (mineral poor) can be exposed to temperatures up to 400°C for long times.

Acknowledgments

The authors would like to acknowledge the EU for funding part of the work through the 6th Framework Program (BIOCOUP, Contract No. 518312). We would like to thank S. R. G. Oudenhoven, C. van Foeken, R. M. Jurgens, and R.M. van Dorp for performing part of the experimental work. We also would like to thank B. Knaken and R.L. Brouwer for building the FB+T-reactor and pilot plant reactor.

Literature Cited

1. Mohan D, Pittman CU, Steeles PH. Pyrolysis of wood/biomass for bio-oil: a critical review. *Energy Fuels*. 2006;20:848–889.
2. Venderbosch RH, Prins W. Review: Fast pyrolysis technology development. *Biofuels Bioprod Bioref*. 2010;4(2):178–208.
3. Czernik S, Bridgwater AV. Overview of applications of biomass fast pyrolysis oil. *Energy Fuels*. 2004;18:590–598.
4. Bridgwater AV. Review of fast pyrolysis of biomass and product upgrading. *Biomass Bioenergy*. 2011. In press.
5. Bridgwater AV, Meier D, Radlein D. An overview of fast pyrolysis of biomass. *Org Geochem*. 1999;30:1479–1493.
6. Kersten SRA, Wang X, Prins W, van Swaaij WPM. Biomass pyrolysis in a fluidized bed reactor. Part 1: literature review and model simulations. *Ind Eng Chem Res*. 2005;44:8773–8785.
7. Venderbosch RH, Prins W. Fast pyrolysis technology development. *Biofuels Bioprod Bioref*. 2010;4:178–208.
8. Haas TJ, Nimlos MR, Donohoe BS. Real-time and post-reaction microscopic structural analysis of biomass undergoing pyrolysis. *Energy Fuels*. 2009;23:3810–3817.
9. Hoekstra E, Hogendoorn JA, Wang X, Westerhof RJM, Kersten SRA, van Swaaij WPM, Groeneveld MJ. Fast pyrolysis of biomass in a fluidized bed reactor: in situ filtering of the vapors. *Ind Eng Chem Res*. 2009;48:4744–4756.
10. Shen J, Wang XS, Garcia-Perez M, Mourant D, Rhodes MJ, Li CZ. Effects of particle size on the fast pyrolysis of oil mallee woody biomass. *Fuel*. 1999;88:1810–1817.
11. Westerhof RJM, Brilman DWF, Van Swaaij WPM, Kersten SRA. Effect of temperature in fluidized bed fast pyrolysis of biomass: oil quality assessment in test units. *Ind Eng Chem Res*. 2010;49:1160–1168.
12. Garcia-Perez M, Wang XS, Shen J, Rhodes MJ, Tian F, Lee WJ, Wu H, Li CZ. Fast pyrolysis of oil mallee woody biomass: effect of temperature on the yield and quality of pyrolysis products. *Ind Eng Chem Res*. 2008;47:1846–1854.
13. Scott DS, Majerski P, Piskorz J, Radlein D. A second look at fast pyrolysis of biomass - the RTI process. *J Anal Appl Pyrolysis*. 1999;51:23–37.
14. Boroson ML, Howard JB, Longwell JP, Peters WA. Heterogeneous cracking of wood pyrolysis tars over fresh wood char surfaces. *Energy Fuels*. 1989;3:735–740.
15. Boroson ML, Howard JB, Longwell JP, Peters WA. Product yields and kinetics from the vapour phase cracking of wood pyrolysis tars. *AIChE J*. 1989;35:120–128.

16. Graham RG, Bergougnout MA, Freil BA. The kinetics of vapour-phase cellulose fast pyrolysis reactions. *Biomass Bioenergy*. 1994;7:33–47.
17. Rath J, Staudinger G. Cracking reactions of tar from pyrolysis spruce wood. *Fuel*. 2001;80:1379–1389.
18. Rath J, Staudinger G. Vapour phase cracking of tar from pyrolysis of birch wood. *Thermal Science*. 2001;5:83–94.
19. Stiles HN, Kandiyoti R. Secondary reactions of flash pyrolysis tars measured in a fluidized bed pyrolysis reactor with some novel design features. *Fuel*. 1989;68:275–282.
20. Baumlin S, Broust F, Ferrer M, Meunier N, Marty E, Lede J. The continuous self stirred tank reactor: measurement of the cracking kinetics of biomass pyrolysis vapours. *Chem Eng Sci*. 2005;60:41–55.
21. Morf P, Hasl P, Nussbaumer T. Mechanisms and kinetics of homogenous secondary reactions of tar from continuous pyrolysis of wood chips. *Fuel*. 2002;81:843–853.
22. Lanza R, Dalle Nogare D, Canu P. Gas phase chemistry in cellulose fast pyrolysis. *Ind Eng Chem Res*. 2009;48:1391–1399.
23. Ahuja P, Kumar S, Singh P.C. A model for primary and heterogeneous secondary reactions of wood pyrolysis. *Chem Eng Technol*. 1996;19:272–282.
24. Scholze B, Meier D. Characterization of the water-insoluble fraction from pyrolysis oil (pyrolytic lignin). Part I. Py-GC/MS, FTIR, and functional groups. *J Anal Appl Pyrolysis*. 2001;60:41–45.
25. Westerhof RJM, Brilman DWF, Garcia-Perez M, Wang Z, Oudenhoven SRG, van Swaaij WPM, Kersten S.R.A. Fractional condensation of biomass fast pyrolysis vapor. *Energy Fuels*. 2011;25:1817–1829.
26. Oasmaa A, Peacocke C. *A Guide to Physical Property Characterization of Biomass Derived Fast Pyrolysis Liquids*, VTT. Technical Research Centre of Finland Espoo; 2001.
27. Hoekstra E, Kersten SRA, Tudos A, Meier D, Hogendoorn J.A. Possibilities and pitfalls in analyzing (upgraded) pyrolysis oil by size exclusion chromatography (SEC). *J Anal Appl Pyrolysis*. 2011;91:76–88.
28. Azeez AM, Meier D, Odermatt J, Willner T. Fast pyrolysis of african and European lignocellulosic biomasses using Py-GC/MS and fluidized bed reactor. *Energy Fuels*. 2010;24:2078–2085.
29. Fahmi R, Bridgwater AV, Donnison I, Yates N, Stones JM. The effect of lignin and inorganic species in biomass on pyrolysis oil yields, quality and stability. *Fuel*. 2008;87:1230–1240.
30. Jensen A, Johansen KD. TG-FTIR Study of the influence of potassium chloride on wheat straw pyrolysis. *Energy Fuels*. 1998;12:929–938.
31. Westerhof RJM, Kuipers NJM, Kersten SRA, van Swaaij WPM. Controlling the water content of biomass fast pyrolysis oil. *Ind Chem Res*. 2007;46:9238–9247.
32. Antal MJ. Effects of reactor severity on the gas-phase pyrolysis of cellulose- and kraft lignin-derived volatile matter. *Ind Eng Chem Prod Res Dev*. 1983;22:366–375.
33. Caballero JA, Font R, Marcilla A. Kinetic study of the secondary thermal decomposition of kraft lignin. *J Anal Appl Pyrolysis*. 1996;38:131–152.
34. Ates F, Putun E, Putun AE. Fast pyrolysis of sesame stalk: yields and structural analysis of bio-oil. *J Anal Appl Pyrolysis*. 2004;71:779–790.
35. Acikgoz C, Onay O, Kockar OM. Pyrolysis Fast pyrolysis of linseed: product yields and compositions. *J Anal Appl*. 2004;71:417–429.
36. DeSisto WJ, Hill N, Beis SH, Mukkamala S, Joseph J, Baker C, Ong TH, Stemmler EA, Wheeler MC, Frederick BG, Heiningen A. Fast Pyrolysis of pine sawdust in a fluidized-bed reactor. *Energy Fuels*. 2010;24:2642–2651.
37. Xianwen D, Chuangzhi W, Haibin L, Yong C. The fast pyrolysis of biomass in CFB reactor. *Energy Fuels*. 2000;14:552–557.
38. Diebold JP, Cernik S, Energy and Fuels. Additives to lower and stabilize the viscosity of pyrolysis oils during storage. *Energy Fuels*. 1997;11:1081–1091.
39. Nanou P, van Rossum G, van Swaaij WPM, Kersten SRA. Evaluation of catalytic effects in gasification of biomass at intermediate temperature and pressure. *Energy Fuels*. 2011;25:1242–1253.
40. Patwardhan PR, Satro JA, Brown RC, Shanks BH. Influence of inorganic salts on the primary pyrolysis products of cellulose. *Bioresour Technol*. 2010;101(12):4646–4655.
41. Patwardhan PR, Brown RC, Shanks BH. Product distribution from the fast pyrolysis of hemicellulose. *ChemSusChem*. 2011;4(5):636–643.
42. Liden AG, Berruti F, Scott DS. A kinetic model for the production of liquids from the flash pyrolysis of biomass. *Chem Eng Comm*. 1988;65:207–221.
43. Shen DK, Gu S, Luo KH, Wang SR, Fang M.X. The pyrolytic degradation of wood-derived lignin from pulping process. *Bioresour Technol*. 2010;101:6136–6146.
44. Shen DK, Gu S. The mechanism for thermal decomposition of cellulose and its main products. *Bioresour Technol*. 2009;100:6496–6504.
45. Shen DK, Gu S, Bridgwater AV. Study on the pyrolytic behavior of xylan-based hemicellulose using TG-FTIR and Py-GC-FTIR. *J Anal Appl Pyrolysis*. 2010;87:199–206.
46. Lin YC, Cho J, Tompsett GA, Westmoreland PR, Huber G.W. Kinetics and mechanism of cellulose pyrolysis. *J Phys Chem*. 2009;113:20097–20107.
47. Oasmaa A, Kuoppala E. Fast pyrolysis of forestry residue.3. Storage stability of liquid fuel. *Energy Fuels*. 2003;17:1075–1084.
48. Uzun BB, Putun AE, Putun E. Composition of products obtained via fast pyrolysis of olive-oil residue: effect of pyrolysis temperature. *J Anal Appl. Pyrolysis*. 2007;79:147–153.
49. Patwardhan PR, Satro JA, Brown RC, Shanks BH. Product distribution from fast pyrolysis of glucose-based carbohydrates. *J Anal Appl Pyrolysis*. 2009;86:323–330.
50. Kawamoto H, Murayama M, Saka S. Pyrolysis behavior of levoglucosan as an intermediate in cellulose pyrolysis: polymerization into polysaccharide as a key reaction to carbonized product formation. *J Wood Sci*. 2003;49:469–473.
51. Branca C, Giudicianni P, Di Blasi C. GC/MS characterization of liquids generated from low-temperature pyrolysis of wood. *Ind Eng Chem Res*. 2003;42:3190–3202.
52. Thurner F, Mann U. Kinetic investigation of wood pyrolysis. *Ind Eng Chem. Process Des Dev*. 1981;20:482–488.
53. Samolada MC, Vasalos IA. A kinetic approach to the flash pyrolysis of biomass in a fluidized bed reactor. *Fuel*. 1991;70:883–889.
54. Meier D, Faix O. State of the art of applied fast pyrolysis of lignocellulosic materials - a review. *Bioresour Technol*. 1999;68:71–77.

Manuscript received Jun. 15, 2011, and revision received Oct. 1, 2011.